JPET Fast Forward. Published on April 27, 2005 as DOI: 10.1124/jpet.105.084418

Zinc activates TREK-2 potassium channel activity

Jin-Sung Kim, Jin-Yong Park, Ho-Won Kang, Eun-Jung Lee, Hyoweon Bang

and Jung-Ha Lee

Department of Life Science (J.S.K., J.Y.P., H.W.K., E.J.L., J.H.L.) and Interdisciplinary Prorgam of Integrated Biotechnology (J.H.L.), Sogang University, Seoul 121-742, Korea; Department of Physiology (H.B.), Chung-Ang University, Seoul, Korea

Running title: Enhancement of human TREK-2 currents by zinc

The name, address, and telephone and fax numbers of the corresponding author:

Jung-Ha Lee, Ph.D.

Department of Life Science, Sogang University,

Mapo-Gu, Sinsu-Dong 1, Seoul 121-742, Korea

Tel) 82-2-705-8791, Fax) 82-2-704-3601

E-mail) **jhleem@ccs.sogang.ac.kr**

The number of text pages: 28 pages

The number of tables: 0

The number of figures: 4 figures

The number of references: 30 references

The number of words in the abstract: 163 words

The number of words in the introduction: 531 words

The number of words in the discussion: 1104 words

A recommended section: Cellular and Molecular

Abbreviations: TREK, TWIK-related K^+ channel; TASK, TWIK-related acid-sensing K^+ channel; TWIK, tandom pore domain weak inwardly rectifying K^+ channel; TALK, TWIK-related alkaline-activated K^+ channel; TRAAK, TWIK-related arachidonic acid-activated K^+ channel; AMV, avian myeloblastosis virus; PCR, polymerase chain reaction; HEPES, 4-(2-hydroxyethyl)-1-piperazineethanesulfonic acid; A, alanine; D, aspartic acid; C, cysteine; E, glutamic acid; H, histidine; N, asparagine

JPET Fast Forward. Published on April 27, 2005 as DOI: 10.1124/jpet.105.084418
This article has not been copyedited and formatted. The final version may differ from this version.

ABSTRACT

TREK-2 is thought to contribute to setting the resting membrane potential and to tuning action potential properties. In the present study, the effects of divalent metal ions (Ba^{2+}, Co^{2+}, Ni^{2+}, Pb^{2+} and Zn^{2+}) were examined on TREK-2 expressed in *Xenopus* oocytes using the two-electrode voltage clamping technique. Pb^{2+} inhibited TREK channel activity (IC_{50} = 15.6 μM), while Zn^{2+} enhanced it in a dose dependent manner (EC_{50} = 87.1 μM). Ba^{2+} slightly inhibited TREK currents, but only at high concentrations. Co^{2+} and Ni^{2+} had no significant effect. The structural element(s) contributing to the zinc enhancement effect were studied using a series of chimeras consisting of Zn^{2+}-activated TREK-2 and Zn^{2+}-inhibited TASK-3. The structural elements were localized to the first pore and the preceding extracellular loop of TREK-2, in which multiple residues including H121, H156, D158, and N177 are likely to be involved in the zinc activation effect. Stimulation by Zn^{2+} may be used as a criterion of TREK-2 distinguishing it from other two-pore K^+ channels.

INTRODUCTION

The tandem-pore K^+ channels have four transmembrane segments and two pore-forming domains in tandem. Because the two-pore K^+ channels are open at resting membrane potential, they are thought to contribute to setting the resting membrane potential in excitable and non-excitable cells. An increase in the activity of the channels can reduce neuronal excitability by hyperpolarizing membrane potential or by reducing the frequency and duration of action potentials. In contrast, a decrease in activity may increase the frequency and duration of action potentials, resulting in enhancing neuronal excitability. Two-pore channels can be differentially modulated by diverse factors including membrane stretching, unsaturated fatty acids, acidic conditions and volatile anesthetics. The two-pore channels are thought to play protective roles in pathological conditions such as ischemia, acidosis, and stroke (Kim, 2003; Lesage and Lazdunski, 2000; Talley et al., 2003).

Molecular studies have revealed that two-pore K^+ channels fall into six subgroups: (i) TWIK channels consisting of TWIK-1 and TWIK-2, (ii) TASK channels consisting of TASK-1, TASK-3, and TASK-5, (iii) TALK channels consisting of TALK-1, TALK-2, and TASK-2, (iv) TRAAK/TREK channels consisting of TREK-1, TREK-2, and TRAAK, (v) THIK channels consisting of THIK-1 and THIK-2, and (vi) TRESK channels consisting of TRESK-1 and TRESK-2. Reconstitution of these channels in expression systems has allowed their individual biophysical and pharmacological properties to be characterized (Kim, 2003; Talley et al., 2003; Franks and Honore, 2004; Kang et al., 2004).

TREK channels generate outwardly rectifying currents that are increased by unsaturated fatty acids such as arachidonic acid, and mechanical stimuli such as cell

swelling, stretch, and positive and negative pressure (Bang et al., 2000; Fink et al., 1996; Maingret et al., 1999). In contrast to voltage-activated K^+ channels, TREK and other two-pore channels are insensitive to traditional K^+ channel blockers such as tetraethylammonium (TEA) and barium (Ba^{2+}) (Kim, 2003). Anesthetics and neuro-protective agents are reported to modulate some two-pore channels, which could therefore be targets for anesthesia and neuro-protection. However, the physiological role of two-pore channels needs to be further investigated, because their reported drug responses are different on distinct K^+ channels. For example, the neuro-protective agents, riluzole and sipatrigine, affect TREK channels in opposite ways: riluzole activates TREK-1 and TRAAK, whereas sipatrigine inhibits them. In addition, TREK-1 and TREK-2 are activated by volatile anesthetics such as halothane and isoflurane, while TRAAK is not (Lesage et al., 2000; Patel et al., 1999). Thus the effects of these drugs are not well enough understood to permit definitive characterization of the physiological functions of the TREK channels (Kim et al., 2001; Maingret et al., 1999; Patel et al., 1998) and specific modulators of the various TREKs are needed.

In the present study we compared the inhibitory effects of several metal ions on human TREK-2 channels (Gu et al., 2002). It turned out that TREK-2 currents were differentially affected by metallic ions; there was potent inhibition by Pb^{2+}, dose-dependent stimulaton by Zn^{2+}, and little effect of the other metal ions. We investigated the structural elements in TREK-2 responsible for Zn^{2+} enhancement using a series of chimeras between Zn^{2+}-activated TREK-2 and Zn^{2+}-inhibited TASK-3. These studies suggested that structures including the first pore and its adjacent extracelluar loop contribute to the Zn^{2+}-mediated enhancement of TREK-2.

MATERIALS AND METHODS

Chemicals: All the chemicals including $CoCl_2$, $NiCl_2$, $PbCl_2$, and $ZnCl_2$ were purchased from Sigma (St. Louis, MO, USA).

Cloning of human TREK-2 and TASK-3 cDNAs: The first strand cDNA was synthesized from 0.5 μg of human brain total RNA (Invitrogen, Carisbad, CA, USA) with AMV reverse transcriptase (Boehringer Mannheim, Indianapolis, IN, USA) by incubating at 42°C for 50 min. The reaction was terminated by heating at 95°C for 5 min. PCR primers were designed from human TREK-2 and TASK-3 sequences (GenBank access numbers, AF385400, AF212829). The forward and reverse primers for human TREK-2 cDNA were 5'-TCTGGGCAACGAAGCA-3' and 5'-AAGCTTGCATTGTCAGCATCAA-3' and for human TASK-3 cDNA were 5'-TGGCGGCCATGAAGAGGCA-3' and 5'-TTTAAACGGACTTCCGGCGTT-3'. The PCR reaction protocol was denaturation at 95°C for 1 min, followed by 30 cycles of 95°C for 30 sec, 54°C for 30 sec, and 72°C for 2 min 30 sec. PCR products were purified and ligated into TOPO TA vector (Invitrogen, Carlsbad, CA, USA). They were identical in sequence to the open reading frames of human TREK-2 and TASK-3 (AF385400, AF212829), and were subcloned in pGEM-HEA to improve expression in Xenopus oocytes (Lee et al., 1999b).

Construction of chimeric channel proteins and TREK-2 mutants: Five chimeras were created by introducing the corresponding regions of TASK-3 into TREK-2 as follows (where the subscripts refer to the regions of TREK-2 substituted): $TREK_{M1M2}$, $TREK_{M3M4}$, $TREK_{P1}$, $TREK_{P1a}$, and $TREK_{P1b}$. The structure of each chimera is shown schematically in Fig. 3. All chimeras were made using a standard PCR overlap extension method (Horton et al., 1989). For $TREK_{M1M2}$, amino acids 1-221 of TREK-2

JPET Fast Forward. Published on April 27, 2005 as DOI: 10.1124/jpet.105.084418
This article has not been copyedited and formatted. The final version may differ from this version.

were replaced by residues 1-143 of TASK-3. For $TREK_{M3M4}$, residues 222-506 of TREK-2 were replaced by residues 144-374 of TASK-3. For $TREK_{P1}$, residues 95-171 of TREK-2 were replaced by residues 31-97 of TASK-3. For $TREK_{P1a}$, residues 95-153 of TREK-2 were replaced by residues 31-79 of TASK-3, and for $TREK_{P1b}$, residues 154-171 of TREK-2 were replaced by residues 80-97 of TASK-3.

TREK-2 mutants (H121A, H135A, H156A, D158A, N177A and N177H) with single point mutations were made by the PCR overlap extension method (Horton et al., 1989) and the mutated regions were confirmed by sequencing.

Expression of TREK-2, TASK-3, and their mutants in Xenopus oocytes: Transcripts were synthesized in vitro using T7 RNA polymerase according to the protocol supplied by the manufacturers (Ambion, Austin, TX, USA), after linearizing the cDNA constructs with *Afl*II. *Xenopus* oocytes were prepared from female *Xenopus laevis* frogs (*Xenopus* One, Ann Arbor, MI, USA), as described previously (Lee et al., 1999a). The oocytes were injected with 0.5-1 ng of cRNA of TREK-2 or TREK-2-like chimeric channels showing activation to zinc, and with 2 ng of cRNA of TASK-3 or TASK-3-like chimeric channels showing inhibition to zinc, using a Drummond Nanoject injector (Parkway, PA, USA). For TREK-2 mutants with single point mutations, 1 ng of cRNA was injected into oocytes to compare their relative expression levels. There was no significant difference between current amplitudes of the mutant channels.

Electrophysiological recordings and data analysis: K^+ currents were measured in SOS solution (in mM: 2 KCl, 100 NaCl, 1.8 $CaCl_2$, 1 $MgCl_2$, 5 HEPES, 2.5 pyruvic acid, 50 μg/ml gentamicin, pH 7.4) using a voltage-clamp amplifier (OC-725C, Warner Instruments, Hamden, CT, USA). Serial zinc solutions were prepared just before experiments by diluting a stock solution of 10 mM $ZnCl_2$ which was made in slightly

acidified SOS, and then diluted zinc solutions were readjusted to pH 7.4 with NaOH. Microelectrodes (Warner Instruments, Hamden, CT, USA) were filled with 3 M KCl and their resistances were 0.2-1.0 MΩ. The currents were sampled at 5 kHz and low pass filtered at 1 kHz using the pClamp system (Digidata 1320A and pClamp 8; Axon instruments, Foster City, CA, USA). Peak currents were analyzed with Clampfit software (Axon instruments, Foster City, CA, USA) and graphical representations of the data were obtained with Prism software (GraphPad, San Diego, CA, USA). Dose-response curves were fitted to the Hill equation: $B = (1 + EC_{50}/[\text{divalent ion}]^{n})^{-1}$, where B is the normalized block, EC_{50} is the concentration of a divalent ion giving half maximal enhancement, and *n* is the Hill coefficient. The concentration of a divalent ion giving half maximal inhibition is represented as IC_{50}. Data are presented as means ± S.E.M. and tested for significance using Student's unpaired *t* test.

JPET Fast Forward. Published on April 27, 2005 as DOI: 10.1124/jpet.105.084418
This article has not been copyedited and formatted. The final version may differ from this version.

RESULTS

The membrane potential of untreated or water-injected oocytes was -22 ± 3 mV in SOS solution containing 2 mM K^+ (n = 12). We first examined the endogenous K^+ currents evoked by a series of test potentials from -120 mV to +20 mV from a holding potential of -90 mV. The currents detected were less than 100 nA even at +20 mV (Fig. 1A,C). In contrast, the membrane potential of oocytes injected with TREK-2 cRNA was -82 ± 4 mV in SOS solution (n = 20, Fig 1C). This hyperpolarization suggests that TREK-2 plays a pivotal role in setting resting membrane potential in cells in which these channels are expressed. Expression of TREK-2 was also evident from the robust outward K^+ currents evoked by depolarizing potentials from a holding potential of -90 mV (Fig 1B). These results suggest that the relatively small current amplitude of the endogenous K^+ currents should have little effect on the biophysical properties of the recombinant TREK-2 currents.

We examined the effects of divalent metal ions on outward K^+ currents evoked every 10 sec by applying test pulses to –20 mV from a holding potential of –90 mV. Perfusion of low concentrations of Ba^{2+} (10, 30, 100 μM) had no effect on the TREK-2 currents, and 300 μM Ba^{2+} only decreased them by about 10 ± 5% (Fig. 1D). Meanwhile, application of concentrations of Ni^{2+} or Co^{2+} up to 300 μM had no effect (Fig. 1E,F). Among of the metal ions examined, only lead (Pb^{2+}) caused substantial inhibition (IC_{50}=15.6 ± 1.5 μM, Fig. 1G), but there was no significant effect of test potential on the extent of inhibition (Fig. 1H). The effects of divalent metal ions were further examined by comparing activation rates of TREK-2 currents before and after application of the ions. The fast time constant (τ_{fast}) of TREK-2 activation was not

significantly changed by any of the divalent ions examined. However, the slow time constant (τ_{slow}) was increased by barium, but not by the other metal ions (Fig. 1I,J).

The application of Zn^{2+} increased the TREK-2 currents in a dose-dependent manner (Fig. 2A,B). The effect was immediate and usually saturated in ~ 1.5 min (Fig. 2B). A similar effect of Zn^{2+} was observed on TREK-2 currents evoked by a ramp protocol (Fig. 2C). Curve fitting gave an EC_{50} of 87.1 ± 3.1 μM and a Hill coefficient *n* of 1.1 ± 0.2 (Fig. 2D). EC_{50} values at different potentials were similar. Consistent with this, the values for percent stimulation of TREK-2 currents by 100 μM zinc were not significantly changed at different test potentials (Fig. 2I), suggesting that Zn^{2+} activation is voltage-independent. The activation time constants, τ_{fast} and τ_{slow}, of the TREK-2 currents tended to be diminished by Zn^{2+}, but the differences were not significant (Fig. 2G,H, $P > 0.05$, Student's *t*-tests).

A key question concerning the Zn^{2+} effect relates to the structural element(s) in TREK-2 that are responsible. To throw light on this question we constructed a series of chimeras between Zn^{2+}-activated TREK-2 and zinc-inhibited TASK-3 (Clarke et al., 2004) cloned from human brain RNA by RT-PCR (see Materials and Methods). Expression of pure TASK-3 channels generated strong outward currents in response to depolarizing potentials, and Zn^{2+} inhibited these currents (IC_{50} = 25.4 ± 1.2 μM, Hill coefficient = 1.0 ± 0.1, Fig. 2E,F). The activation time constants (τ_{fast} and τ_{slow}) of TASK-3 were elevated by 100 and 1000 μM Zn^{2+} (Fig. 2G,H, $P < 0.01$, 0.05, Student's *t*-test). The percent inhibition of the TASK-3 currents by 100 μM Zn^{2+} was similar at different potentials, suggesting that Zn^{2+} inhibition of TASK-3 is voltage-independent (Fig. 2I).

JPET Fast Forward. Published on April 27, 2005 as DOI: 10.1124/jpet.105.084418
This article has not been copyedited and formatted. The final version may differ from this version.

To help identify the site(s) modulated by Zn^{2+}, chimeras were first constructed by substituting either the N-terminal or C-terminal halves of TREK-2 with the corresponding regions of TASK-3. Expression of $TREK_{M1M2}$ (first half of TREK-2 replaced with that of TASK-3), gave strong outward currents inhibited by Zn^{2+} (IC_{50}=27.7 ± 2.0 μM, Fig. 3B). The $TREK_{M1M2}$ currents were activated instantaneously in response to step test potentials; consequently the activation kinetics were not properly fitted by exponential equations. Apparently replacement of the first half of TREK-2 with that of TASK-3 creates a chimera that is activated much faster than wild type TREK-2 or TASK-3A.

In contrast, expression of $TREK_{M3M4}$ (second half of TREK-2 replaced with that of TASK-3) did not generate significant outward currents so that we could not evaluate the effect of Zn^{2+} ions (Fig. 3C). However, the fact that the Zn^{2+} sensitivity of the first-half chimera ($TREK_{M1M2}$) resembled that of TASK-3 suggests that the N-terminal half of TREK-2 plays an important role in controlling the enhancement by Zn^{2+}.

We further dissected the first half of TREK-2 to localize the element(s) influencing the Zn^{2+} enhancement effect. Our hypothesis was that the first pore and/or its neighboring extracellular loop would be more important for the Zn^{2+} effect than the transmembrane or cytoplasmic loops. Accordingly, we constructed $TREK_{P1}$ (the first pore loop and preceding extracellular loop of TREK-2 replaced by those of TASK-3) and examined its response to Zn^{2+}. Superfusion of Zn^{2+} solution inhibited channel activity (Fig. 3D) with an IC_{50} of 12.6 ± 2.1 μM, about 2 fold lower than that for TASK-3. These data support the idea that the first pore and the preceding extracellular loop are responsible for the opposing effects of Zn^{2+} on TREK-2 and TASK-3. The reason why

substitution of the TASK-3 regions actually renders $TREK_{P1}$ more sensitive to Zn^{2+} than TASK-3 itself remains to be investigated.

To further localize the key controlling structures, we constructed $TREK_{P1a}$ and $TREK_{P1b}$ (the extracellular loop and first pore of TREK-2, respectively, replaced by the corresponding regions of TASK-3) (Fig. 3 E,F). Zn^{2+} inhibited the activity of $TREK_{P1a}$ with an IC_{50} of 32.6 ± 2.6 μM, whereas 58% of $TREK_{P1a}$ activity was maintained at 1000 μM zinc (Fig. 3E). These results indicate that introduction of the extracellular loop of TASK-3 causes $TREK_{P1a}$ to be partially inhibited by Zn^{2+} rather than strongly enhanced by it. It also implies that the extracellular loop of TREK-2 contributes to the Zn^{2+} modulation effect. The outcome with the other chimera, $TREK_{P1b}$, was similar, with an IC_{50} of 29.6 ± 2.2 μM (Fig. 3F). Incomplete inhibition (~34%) at more than 1000 μM Zn^{2+} was also found with $TREK_{P1b}$. The levels of residual inhibition in $TREK_{P1a}$ and $TREK_{P1b}$ suggest that the first pore is more important than the intracellular loop for the enhancement of TREK-2 channel activity by Zn^{2+}. The activation time constants (τ_{fast} and τ_{slow}) of the chimeric channels are shown as a function of Zn^{2+} concentration in Fig. 3G. No significant difference was found between the fast activation time constants of the chimeras in either the presence or absence of Zn^{2+}. The slow activation constants of the three mutant channels in the absence of Zn^{2+} were similar and significantly lower than that of wild-type TREK-2 ($P<0.05$, Student's *t*-test, Figs. 2H, 3G). The slow constants of $TREK_{P1}$ and $TREK_{P1b}$ were increased by Zn^{2+}, while that of $TREK_{P1a}$ was unaffected (Fig. 3G).

Zn^{2+} can interact with histidine (H) and cysteine (C) residues, and the acidic amino acids, aspartic acid (D) and glutamic acid (E). These types of residue are present in the extracellular loop; we examined the roles of the three histidine residues (H121,

JPET Fast Forward. Published on April 27, 2005 as DOI: 10.1124/jpet.105.084418
This article has not been copyedited and formatted. The final version may differ from this version.

H135 and H156) by replacing them individually with alanine (A). $TREK_{H121A}$ activity was increased by 10 μM Zn^{2+}, and somewhat further by 100 μM Zn^{2+}. Thereafter there was partial inhibition by 1000 μM Zn^{2+}, activity dropping to about the level produced by 10 μM zinc. Similarly, $TREK_{H156A}$ activity was enhanced by 10 μM Zn^{2+}, but was not further increased by 100 μM Zn^{2+}, and was partially inhibited by 1000 μM Zn^{2+} (Fig. 4B); the level of the inhibited activity tended to be slightly lower than the control activity in the absence of Zn^{2+}. These biphasic profiles suggest that H121 and H156 in the extrafacial loop contribute to activation by Zn^{2+}. Unlike $TREK_{H121A}$ and $TREK_{H156A}$, however, $TREK_{H135A}$ was activated by Zn^{2+}, and its activation profile was similar to that of wild type TREK-2. Therefore, of the three histidine residues, H121 and H156 seem to be critical for Zn^{2+} activation.

In the first pore region, we selected D158 and N177 (asparagine177) and individually mutated them to alanine (A), because D158, an acidic amino acid, was recently reported to play a role in Cu^{2+} activation of TREK-1 (Gruss et al., 2004), and N177 corresponds to H98 of TASK-3, which is essential for Zn^{2+} inhibition of TASK-3 (Clarke et al., 2004). $TREK_{D158A}$ activity was stimulated by Zn^{2+} up to 100 μM, and its Zn^{2+} activation profile was similar to that of wild type TREK-2 over that range. However there was no further activation, but rather slight inhibition, by 1000 μM Zn^{2+}. The fold activations of $TREK_{D158A}$ by 100 and 1000 μM Zn^{2+} were greater than those of $TREK_{H121A}$ or $TREK_{H156A}$. Nevertheless, the partial inhibition of $TREK_{D158A}$ by 1000 μM Zn^{2+} suggests that D158 may participate in Zn^{2+} activation of TREK-2, though it may be less important than H121 and H156. Similarly, the activities of $TREK_{N177A}$ and $TREK_{N177H}$ were stimulated by low concentrations of Zn^{2+} up to 100 μM, and then

partially inhibited by 1000 μM Zn^{2+}, and the fold stimulations by 1000 μM Zn^{2+} were less than that of wild type TREK-2 ($P<0.05$, Student *t*-test, Fig. 4B), implying that N177 also participates in Zn^{2+} stimulation.

These mutagenesis experiments suggest that multiple residues spreading across the extracellular loop and first pore contribute to Zn^{2+} activation of TREK-2. Although H121 and H156 in the extracellular loop and D158 and N177 in the first pore contribute to Zn^{2+} activation, we cannot rule out the possibility that residues in other regions contribute to the activation.

DISCUSSION

We have compared the effects of various divalent metal ions on the human TREK-2 channel expressed in *Xenopus* oocytes. Of the metal ions, only Zn^{2+} enhanced channel activity. Examination of chimeras of TREK-2 and TASK-3, which are affected in opposite directions by Zn^{2+}, showed that structural elements in the extracellular loop and first pore are involved in Zn^{2+} stimulation. Substitution of H121 and H156 in the extracellular loop and of D158 and N177 in the first pore rendered the dose-dependent enhancement effect somewhat biphasic, with less activation at higher Zn^{2+} concentrations. This indicates that H121, H156, D158, and N177 contribute to Zn^{2+} activation. However, none of the substitutions totally abolished TREK-2 channel stimulation by Zn^{2+}.

Using the information obtained concerning the role of these residues, we attempted to abolish Zn^{2+} activation of TREK-2, or convert it to Zn^{2+} inhibition, by introducing additional single point mutation(s). Mutation of N177, in the pore, to histidine, the corresponding residue in TASK-3, gave a biphasic modulation effect similar to that with N177A. In addition, even when H156A and N177A were combined, the Zn^{2+} modulation profile resembled that of H156A and N177A. Furthermore, H121 and H156 are identical to the residues in the TREK-1 channel (Fig. 4A), which is reported to be inhibited by Zn^{2+} (Gruss et al., 2004). These findings suggest that the zinc activation effect is not due to one or two residues, but that multiple residues including the four residues identified here and unidentified residues are likely to be jointly responsible. For example, negatively charged residues (D and E) in the extracellular loop could be also targets for the effect of Zn^{2+}. Therefore, it will be of interest to establish how a number of different residues interact to bring about Zn^{2+} activation.

Structure-function studies of TREK and other two-pore channels have revealed the critical regions required for sensitivity to free fatty acids and pH, by analyzing deletion mutants and chimeric channels (Kim, 2003; Franks and Honore, 2004). The initial 30-amino acid regions of the carboxyl termini of TREK-1 and TREK-2 were identified as crucial for activation by free fatty acids and protons. A glutamate residue in the region was shown to play a role as a proton sensor that also affects the sensitivity to mechanic stimuli and free fatty acids. The same C-terminal region of TREK-1 was shown to participate in its activation by volatile anesthetics such as halothane. In contrast to the carboxyl termini involved in sensitivity to pH and fatty acids, the regions affected by divalent ions were localized to the first pore segment and the preceding extra-facial loop. E70 in the extrafacial loop of TASK-1 was shown to be critical for inhibition by ruthenium red (Czirjak and Enyedz, 2003). In the case of TASK-3, E70 in the extrafacial loop and H98 in the first pore were critical for zinc inhibition (Gruss et al., 2004). These results in combination with our findings suggest that the extracelluar loop and the first pore contain key motif(s) participating in the modulation of two-pore K^+ channel activity by endogenous trace ions such as Zn^{2+} and Cu^{2+}. Therefore, these regions are potential targets for drugs regulating two-pore channel activity.

Like TREK-2, acid sensing ion channels and ATP-sensitive K^+ channels show Zn^{2+}-mediated activation (Baron et al., 2001; Prost et al., 2004). Zn^{2+} potentiates acid sensing channels activated by protons, and the Zn^{2+}-interacting sites were identified as H163 and H339 in the extracelluar loop located just after the first trans-membrane domain. Zn^{2+} activates ATP-sensitive K^+ channels by interacting with extracellular H326 and H332 of the SUR (sulphonylurea receptor) subunit (Bancila et al., 2005). Although issues such as Zn^{2+}-interacting sites have been solved, it still remains to be

determined how Zn^{2+} activates channels. For example, it may modulate either the number of channels in the membrane, their single channel conductance, or their probability of opening. Single channel recordings in the outside-out configuration might distinguish between these possibilities. In the case of shaker- and shaw-type K^+ channels, Zn^{2+} activates channel activity by increasing subunit tetramerization (Jahng et al., 2001; Strang et al., 2003). Therefore, the question whether the Zn^{2+} activation effect on TREK-2 is correlated with dimerization of its subunits should be tested by biochemical approaches.

Cu^{2+} has been shown to activate TREK-1 (Gruss et al., 2004) and D128 plays a critical role in this effect. Therefore, we have tested whether Cu^{2+} stimulates TREK-2 activity. Application of Cu^{2+} led to activation of TREK-2 with an activation profile similar to that of Zn^{2+} (Kim, Bang, and Lee, unpublished data).

In the brain, Zn^{2+} is stored in synaptic vesicles and released from presynaptic terminals by depolarization (Ebadi et al., 1994; Howell et al., 1984). The released Zn^{2+} reaches a concentration exceeding 100 μM upon strong synaptic activation, and interacts with structures such as ion channels and ligand-gated receptors to modulate synaptic transmission and neuronal excitability. Hence, TREK-2 may be one of the targets modulated by elevated Zn^{2+} concentrations. The Zn^{2+} activation effect could be a mechanism by which Zn^{2+} modulates neuronal excitability. In addition, it may help, together with other factors such as membrane stretching, un-saturated fatty acids and hydrogen ions, to protect neurons from damage under pathological conditions, by attenuating neuronal excitability. Conversely, Zn^{2+} deficiency may depolarize the membranes of neuronal cells expressing TREK-2, thus aggravating the damage to them under pathological conditions by increasing their excitability.

JPET Fast Forward. Published on April 27, 2005 as DOI: 10.1124/jpet.105.084418
This article has not been copyedited and formatted. The final version may differ from this version.

Unlike Zn^{2+}, Pb^{2+} proved to be a strong inhibitor of TREK-2 activity, while Co^{2+} and Ni^{2+} had no effect (Fig. 1). Pb^{2+} blocks voltage-gated Ca^{2+} and K^+ channels and hyperpolarization-activated channels, but activates SK4, a Ca^{2+}-activated K^+ channel by acting as a Ca^{2+} surrogate. These findings suggest that Pb^{2+} acts differently on different ion channels (Cao and Houamed, 1999; Atchison, 2003; Dai et al, 2003; Liang et al, 2004). Therefore, its effects may differ between different types of two-pore K^+ channels. Together with the absence of effect of Co^{2+} and Ni^{2+}, the effect of Pb^{2+} might be used to distinguish TREK-2 from other two-pore K^+ channels.

Recently, Clarke et al. (2004) showed that Zn^{2+} strongly inhibits human TASK-3 with an IC_{50} = 19.8 μM, but has no effect on human TASK-1 and TASK-2. Gruss et al. (2004) have also shown that Zn^{2+} inhibits TASK-3, with an IC_{50} = 12.7 μM, and that the IC_{50} for TREK-1 was 659 μM. In the light of these reports and our findings, it seems that the effect of Zn^{2+} could be used as a criterion to distinguish TREK-2 from TREK-1 and other two-pore channels, although the effect of Zn^{2+} on other two-pore K^+ channels remains to be investigated. In addition, the results reported here provide a basis for exploring the pore structure and function of two-pore potassium channels.

ACKNOWLEDGEMENT

We thank Drs. Donghee Kim and Edward Perez-Reyes for their helpful comments on this paper. Jin-Sung Kim and Jin-Yong Park contributed equally to this work.

REFERENCES

Atchison WD (2003) Effects of toxic environmental contaminants on voltage-gated calcium channel function: from past to present. *J Bioenerg Biomembr* **35**:507-532.

Bang H, Kim Y, and Kim D (2000) TREK-2, a new member of the mechanosensitive tandem-pore K+ channel family. *J Biol Chem* **275**:17412-17419.

Bancila V, Cens T, Monnier D, Chanson F, Faure C, Dunant Y, and Bloc A (2005) Two SUR1-specific Histidine residues mandatory for zinc-induced Activation of the Rat K_{ATP} channel. *J Biol Chem* **280**:8793-8799.

Baron A, Schaefer L, Lingueglia E, Champigny G, and Lazdunski M (2001) Zn^{2+} and H^{+} are coactivators of acid-sensing ion channels. *J Biol Chem* **276**:35361-35367.

Cao YJ and Houamed KM (1999) Activation of recombinant human SK4 channels by metal cations. *FEBS Lett* **446**:137-141.

Czirjak G and Enyedz P (2003) Ruthenium red inhibits TASK-3 potassium channel by interconnecting glutamate 70 of the two subunits. *Mol Pharmacol* **63**:646-652.

Clarke CE, Veale EL, Green PJ, Meadows HJ, and Mathie A (2004) Selective block of the human 2-P domain potassium chnnel, TASK-3, and the native leak potassium current, IKSO, by zinc. *J Physiol* **560**:51-62.

Dai XQ, Karpinski E, and Chen XZ (2003) Pb^{2+} inhibits the hyperpolarization-activated current in acutely isolated dorsal root ganglion neurons. *Neuroscience* **120**:57-63.

Ebadi M, Elsayed MA, and Aly MH (1994) The importance of zinc and metallothionein in brain. *Biol Signals* **3**:123-126.

Fink M, Duprat F, Lesage F, Reyes R, Romey G, Heurteaux C, and Lazdunski M (1996) Cloning, functional expression and brain localization of a novel unconventional outward rectifier K^+ channel. *EMBO J* **15**:6854-6862.

Franks NP and Honore E (2004) The TREK K2P channels and their role in general anaesthesia and neuroprotection. *Trends Pharmacol Sci* **25**:601-608.

Gruss M, Mathie A, Lieb WR, and Franks NP (2004) The two-pore-domain K(+) channels TREK-1 and TASK-3 are differentially modulated by copper and zinc. *Mol Pharmacol* **66**:530-537.

Gu W, Schlichthorl G, Hirsch JR, Engels H, Karschin C, Karschin A, Derst C, Steinlein OK, and Daut J (2002) Expression pattern and functional characteristics of two novel splice variants of the two-pore-domain potassium channel TREK-2. *J Physiol* **539:**657-668.

Horton RM, Hunt HD, Ho SN, Pullen JK, and Pease LR (1989) Engineering hybrid genes without the use of restriction enzymes: gene splicing by overlap extension. *Gene* **77**:61-68.

Howell GA, Welch MG, and Frederickson CJ (1984) Stimulation-induced uptake and release of zinc in hippocampal slices. *Nature* **308**:736-738.

Jahng AW, Strang C, Kaiser D, Pollard T, Pfaffinger P, Choe S (2002) Zinc mediates assembly of the T1 domain of the voltage-gated K channel 4.2. *J Biol Chem* **277**:47885-47890.

Kang D, Mariash E, and Kim D (2004) Functional expression of TRESK-2, a new member of the tandem-pore K^+ channel family. *J Biol Chem* **279**:28063-28070.

Kim D (2003) Fatty acid-sensitive two-pore domain K^+ channels. *Trends Pharmacol Sci* **24**:648-654.

Kim Y, Gnatenco C, Bang H, and Kim D (2001) Localization of TREK-2 K^+ channel domains that regulate channel kinetics and sensitivity to pressure, fatty acids and pHi. *Eur J physiol* **442**:952-960.

Lee JH, Daud AN, Cribbs LL, Lacerda AE, Pereverzev A, Klöckner U, Schneider T, and Perez-Reyes E (1999a) Cloning and expression of a novel member of the low voltage-activated T-type calcium channel family. *J Neurosci* **19**:1912-1921.

Lee JH, Gomora JC, Cribbs LL, and Perez-Reyes E (1999b) Nickel block of three cloned T-type calcium channels: low concentrations selectively block alpha1H. *Biophys J* **77**:3034-3042.

Lesage F and Lazdunski M (2000) Molecular and functional properties of two-pore domain potassium channels. *Am J Physiol Renal* **279**:F793-801.

Lesage F, Terrenoire C, Romey G, and Lazdunski M (2000) Human TREK2, a 2Pdomain mechano-sensitive K^+ channel with multiple regulations by polyunsaturated fatty acids, Lysophospholipids, and G_s, G_i, and G_q protein-coupled Receptors. *J Biol Chem* **275**:28398-28405.

Liang GH, Jarlebark L, Ulfendahl M, Bian JT, and Moore EJ (2004) Lead (Pb^{2+}) modulation of potassium currents of guinea pig outer hair cells. *Neurotoxicol Teratol* **26**:253-260.

Maingret F, Patel AJ, Lesage F, Lazdunski M, and Honore E (1999) Mechano- or acidstimulation, two interactive modes of activation of the TREK-1 potassium channel. *J Biol Chem* **274**:26691-26696.

Patel AJ, Honore E, Maingret F, Lesage F, Fink M, Duprat F, and Lazdunski M (1998) A mammalian two pore domain mechano-gated S-like K^+ channel. *EMBO J* **17**:4283-4290.

Patel AJ, Honore E, Lesage F, Fink M, Romey G, and Lazdunski M (1999) Inhalational anesthetics activate two-pore-domain background K^+ channels. *Nat Neurosci* **2**:422-426.

Prost AL, Bloc A, Hussy N, Derand R, and Vivaudou M (2004) Zinc is both an intracellular and extracellular regulator of KATP channel function. J Physiol (Lond) **559:**157-167.

Strang C, Kunjilwar K, DeRubeis D, Peterson D, Pfaffinger PJ (2003) The role of Zn^{2+} in Shal voltage-gated potassium channel formation. *J Biol Chem* **278**:31361-31371.

Talley EM, Sirois JE, Lei Q, and Bayliss DA (2003) Two-pore-domain (KCNK) potassium channels: dynamic roles in neuronal function. *Neuroscientist* **9**:46-56.

Footnotes

Financial support: This work was supported by a special grant from Sogang University to Jung-Ha Lee.

JPET Fast Forward. Published on April 27, 2005 as DOI: 10.1124/jpet.105.084418
This article has not been copyedited and formatted. The final version may differ from this version.

Legend for Figures

Figure 1. Effects of metal ions on human TREK-2 currents. Representative native K^+ currents (A) and human recombinant TREK-2 currents (B) were recorded from oocytes in which H_2O and TREK-2 cRNA was injected, respectively. Currents were evoked by a series of step potentials ranging from -120 mV to +20 mV, from a holding potential of -90 mV. The average current-voltage relationships of native K^+ channels and TREK-2 channels were plotted (C, n = 12, 20). K^+ currents through TREK-2 were evoked by test potentials to –20 mV for 200 msec from a holding potential of –90 mV to examine the effects of divalent metal ions on TREK-2. Currents were recorded every 10 sec with 2 mM K+ as charge carrier in the presence and absence of increasing concentrations of Ba^{2+} (D, ●), Ni^{2+} (E, ○), Co^{2+} (F, ▲), and Pb^{2+} (G, △). D-G, All currents were normalized to the control currents elicited in the absence of metal ions and plotted as a function of metal ion concentration. In each inset, representative TREK-2 currents in the absence (control) and presence (asterisk) of a 300 μM metal ion solution are overlapped to show the effect of each metal ion on TREK-2. The vertical bars in the insets represent 1 μA. Data are represented as means ± SEM (n = 6-8). The smooth curve for Pb2+ blockade was fitted using the Hill equation (see Materials and Methods). The estimated IC_{50} of Pb^{2+} on the TREK-2 current is 15.6 ± 1.5 μM (n = 6). Inhibition percentages of TREK-2 currents by 30 μM Pb^{2+} were plotted against potentials (H, n = 6). The activation time constants (τfast and τslow) of TREK-2 currents were obtained from fitting each current trace with two-exponential curves, and their average values were plotted against concentrations (I,J). Except for Ba^{2+}, the other metal ions did not change activation time constants significantly (n = 6-8).

Figure 2. Effects of Zn^{2+} on TREK-2 and TASK-3 currents. The same voltage protocol as in Fig. 1 was applied to evoke TREK-2 and TASK-2 currents every 10 sec (A, B, D-F). The vertical bars represent 1 μA. A, Representative TREK-2 current traces in the presence and absence of increasing concentrations of Zn^{2+} are overlapped. B, A representative time course of Zn^{2+} stimulation of TREK-2 currents. Peak TREK-2 currents in response to increasing concentrations of Zn^{2+} are plotted against time (sec). The TREK-2 currents have been normalized to the control current before application of Zn^{2+}, and then the normalized current amplitude (fold) plotted against time (sec). C, The Zn^{2+} enhancement effect on the TREK-2 current is voltage-independent. TREK-2 currents were evoked by a ramp protocol with potential changed from -120 to +20 mV for 200 msec. Stimulation of the TREK-2 current by Zn^{2+} was essentially voltage independent. D, Dose–response curve of the Zn^{2+} enhancement of TREK-2. Peak TREK-2 currents were normalized to the control currents in the absence of Zn^{2+} and the fold stimulation is plotted against Zn^{2+} concentration. The smooth curve was obtained by fitting the data using the Hill equation. The estimated EC_{50} on TREK-2 is 87.1 ± 3.1 (μM) and a Hill coefficient is 1.1 ± 0.2 (means ± SEM, n = 8). E, Zn^{2+} inhibition of TASK-3 currents. The voltage protocol used in Fig. 2A was applied to elicit TASK-3 currents every 10 sec, and the currents before and after application of Zn^{2+} are overlapped. F, Dose-response curve of the Zn^{2+} inhibition of TASK-3. The smooth curves were obtained by fitting data using the Hill equation. The estimated IC_{50} and Hill coefficient of Zn^{2+} inhibition on TASK-3 currents is 25.4 ± 1.2 μM and 1.0 ± 0.1 (n = 6). G & H, The activation time constants (τ_{fast} and τ_{slow}) of TREK-2 (●) and TASK-3 (○) currents were obtained from fitting them with two-exponential curves, and then plotted against zinc concentrations (n = 8,6). I, Voltage-dependency of TREK-2 (●) activation

JPET Fast Forward. Published on April 27, 2005 as DOI: 10.1124/jpet.105.084418
This article has not been copyedited and formatted. The final version may differ from this version.

and TASK-3 (○) inhibition by 100 μM zinc was shown by plotting their average percent values against test potentials (n = 8,6).

Figure 3. Effect of Zn^{2+} on chimeras of the TREK-2 and TASK-3 channels. A, Schematic diagrams of TREK-2 and TASK-3. White cylinders and thin lines indicate regions derived from TREK-2, grey cylinders and thick lines do those derived from TASK-3. P1 between M1 and M2 is divided into two portions, the extracellular loop (P1a) and the first pore (P1b), and P2 between M3 and M4 is the second pore (see methods). B-F, Zn^{2+} inhibition profiles of $TREK_{M1M2}$ (B, ●), $TREK_{M3M4}$ (C), $TREK_{P1}$ (D, ○), $TREK_{P1a}$ (E, ▲), and $TREK_{P1b}$ (F, △). In the left panels are schematic diagrams of the chimeras. In the middle panels, representative currents of each chimera recorded in the absence (control) and presence of serial concentrations of Zn^{2+} are overlapped. All the currents were evoked by the same voltage protocol every 10 sec. Vertical bars represent 1 μA. In the right panels, all the currents are normalized to the control current recorded in the absence of Zn^{2+} and plotted against the applied Zn^{2+} concentration. The smooth curves were fitted using the Hill equation. The estimated IC_{50} values of $TREK_{M1M2}$, $TREK_{P1}$, $TREK_{P1a}$, and $TREK_{P1b}$ are 27.7 ± 2.0, 12.6 ± 2.1, 32.6 ± 2.0, and 29.6 ± 2.2 μM and their Hill coefficients are 1.5 ± 0.06, 1.0 ± 0.07, 1.2 ± 0.19, 1.3 ± 0.1, respectively (n = 5-7). C, No functional expression of $TREK_{M3M4}$ was detected. G, Activation time constants of chimeric channels. Chimeric channel currents were fitted with two exponential curves and their fast and slow time constants (τ_{fast} and τ_{slow}) were plotted against zinc concentrations (n = 4-6).

JPET Fast Forward. Published on April 27, 2005 as DOI: 10.1124/jpet.105.084418
This article has not been copyedited and formatted. The final version may differ from this version.

Figure 4. The effect of Zn^{2+} on TREK-2 mutants. A, Sequence alignment of human TREK-2, TREK-1 and TASK-3 in the extracellular loop (P1a) and the first pore (P1b). The histidine residues in bold, H121, H135, and H156, in the extracellular loop of TREK-2 were individually mutated to alanine. In the pore region underlined, D158 of TREK-2 was mutated to alanine and D177 was mutated to alanine or histidine. B, The effect of Zn^{2+} on $TREK_{H121A}$ (□), $TREK_{H135A}$ (■), $TREK_{H156A}$ (○), $TREK_{D158A}$ (●), $TREK_{N177A}$ (△), and $TREK_{N177H}$ (▲). Currents through the mutant channels were evoked by application of -20 mV from a holding potential of -90 mV every 10 sec. Representative current traces of individual mutant channels before an after application of serial zinc solutions were displayed and normalized current amplitudes are plotted against Zn^{2+} concentrations. Data represent means ± SEM (n = 4-8). C, Activation time constants of mutant channel currents before and after application of serial zinc solutions. Activation of each current was fitted with double exponential curves and activation time constants (τ_{fast} and τ_{slow}) were plotted (n = 4-8).

JPET Fast Forward. Published on April 27, 2005 as DOI: 10.1124/jpet.105.084418
This article has not been copyedited and formatted. The final version may differ from this version.

Figure 1

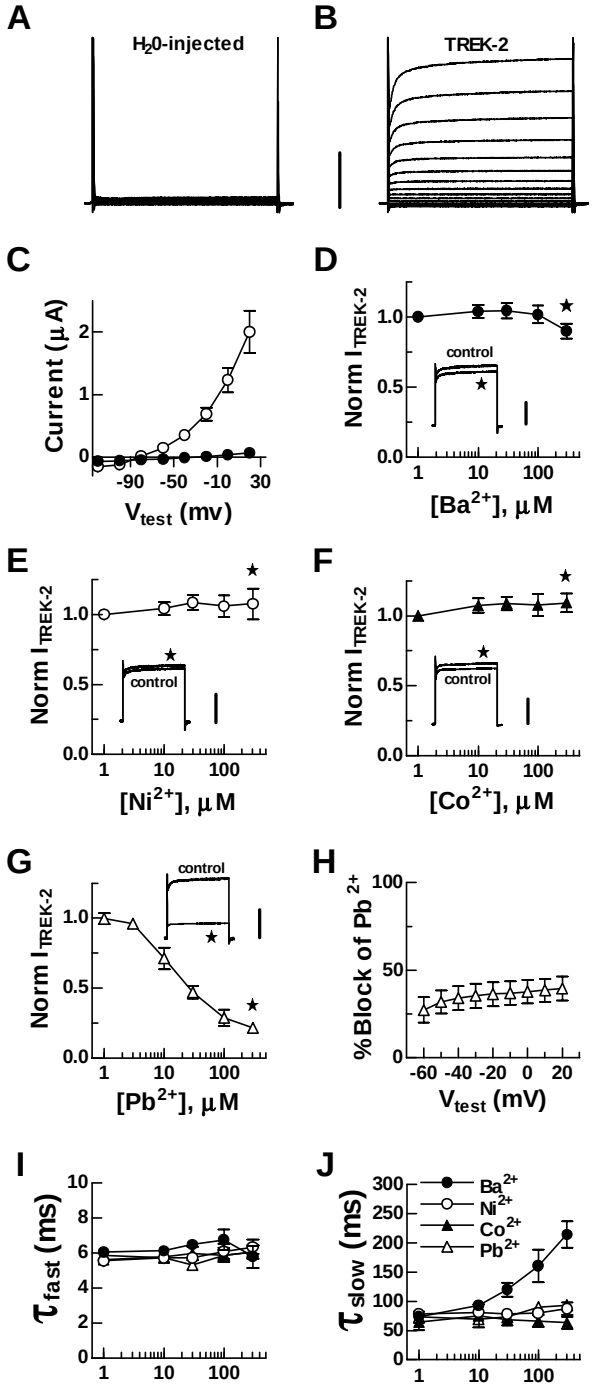

JPET Fast Forward. Published on April 27, 2005 as DOI: 10.1124/jpet.105.084418
This article has not been copyedited and formatted. The final version may differ from this version.

Figure 2

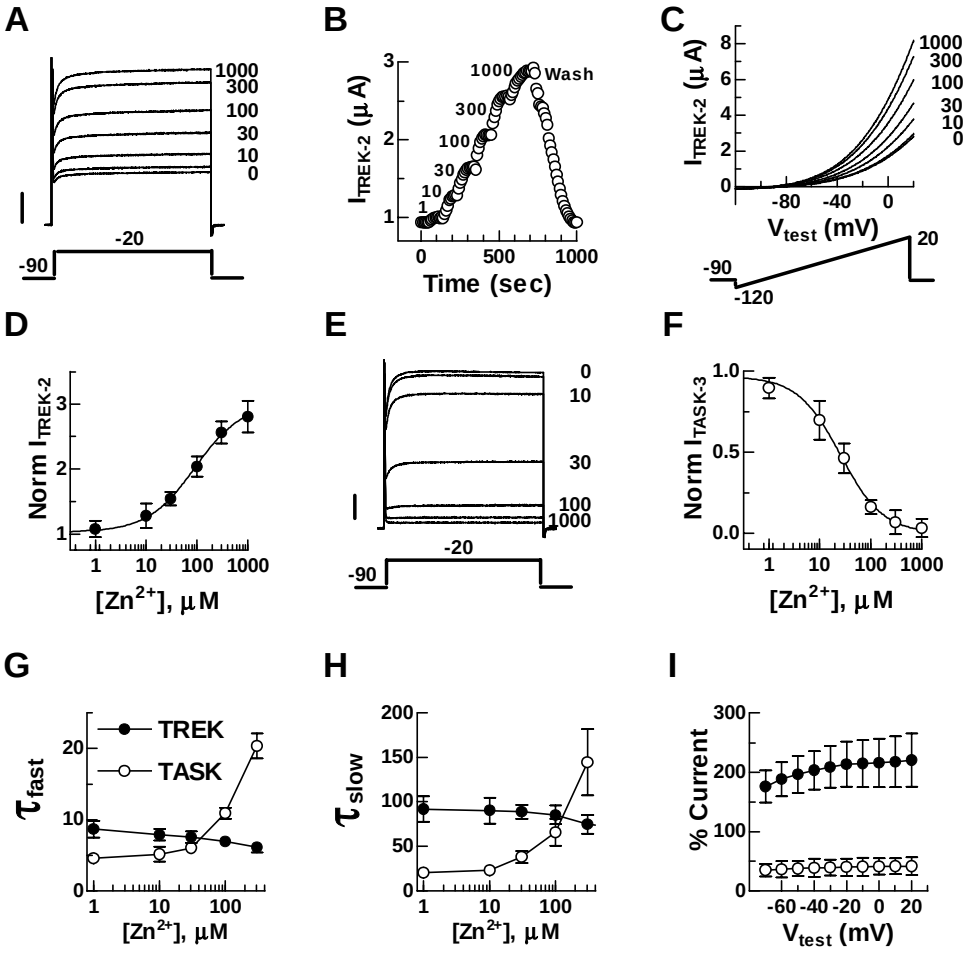

JPET Fast Forward. Published on April 27, 2005 as DOI: 10.1124/jpet.105.084418
This article has not been copyedited and formatted. The final version may differ from this version.

Figure 3

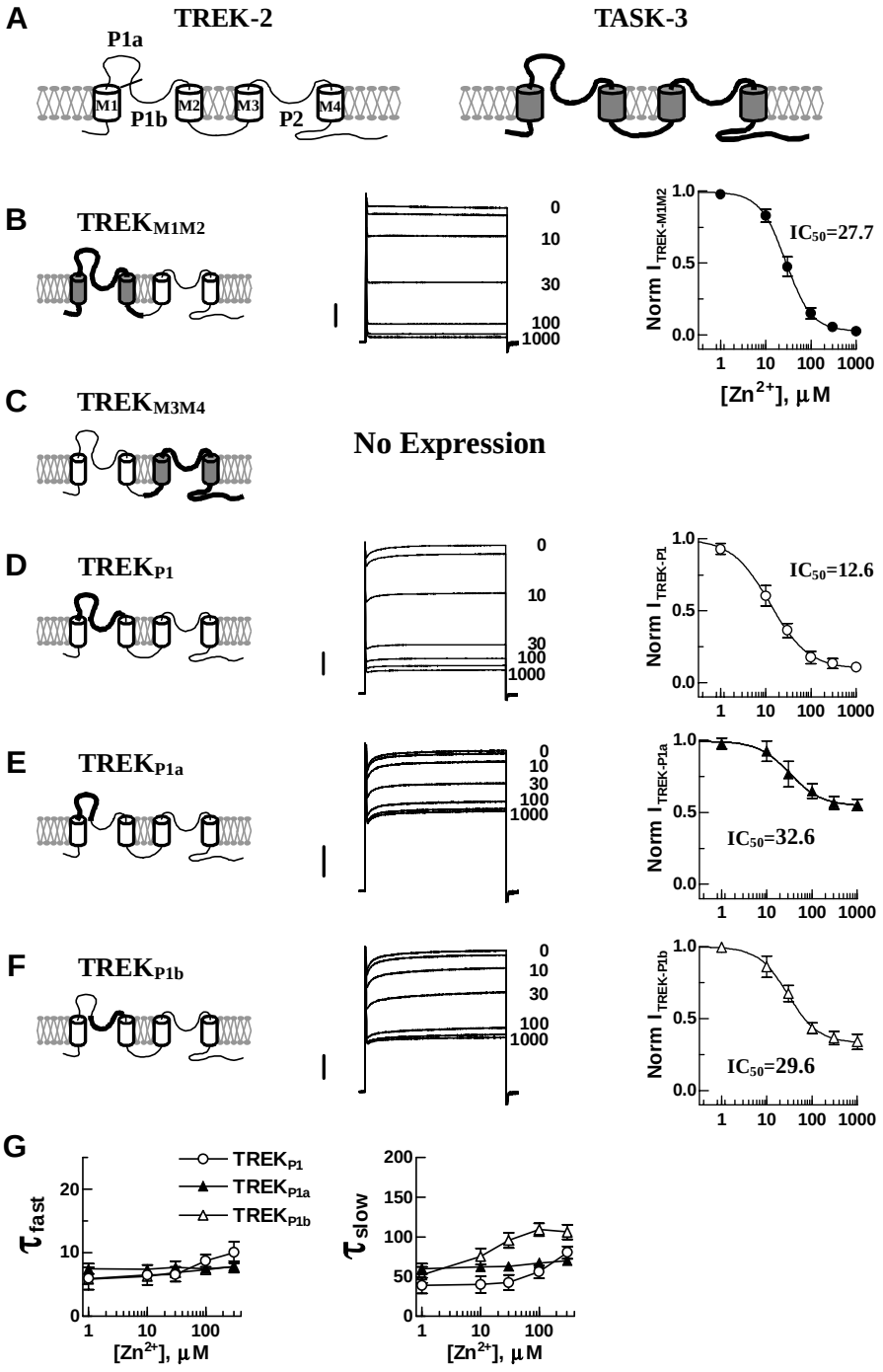

JPET Fast Forward. Published on April 27, 2005 as DOI: 10.1124/jpet.105.084418
This article has not been copyedited and formatted. The final version may differ from this version.

Figure 4